Polymorphs of Oxotitanium Phthalocyanine and Their Applications for Photoreceptors

T. Enokida

Graduate School of Science and Technology, Chiba University, 1-33 Yayoi-cho, Chiba-shi 260, Japan

R. Hirohashi

Faculty of Engineering, Chiba University, 1-33 Yayoi-cho, Chiba-shi 260, Japan

T. Nakamura

Faculty of Engineering, Shizuoka University, 3-5 Johoku, Hamamatsu-shi 432, Japan

Polymorphs of oxotitanium phthalocyanine (TiOPc) and their application as charge generation materials in multilayered photoreceptors are investigated. TiOPc has five typical polymorphs, and their differences can be seen in x-ray powder diffraction patterns, IR and visible absorption spectra, and electron spin resonance spectra. These photoreceptor devices show good electrophotographic properties. A photoreceptor of γ-TiOPc/butadiene derivative exhibited dark decay = 54 V/sec, $E_{1/2}$ = 1.8 ergs/cm^2, and surface voltage with 790-nm irradiation at 5 ergs/cm^2 = −35 V, at 10 ergs/cm^2 = −30 V, and at 30 ergs/cm^2 = −25 V.

Journal of Imaging Science 34: 234–242 (1990)

Introduction

Phthalocyanine compounds are a very interesting class of organic materials, because of their highly functional properties in scientific fields.[1] Many investigations have been reported on the preparation of phthalocyanine coloring materials for printing inks, paints and plastics. In the past twenty years, phthalocyanines have been found to be promising materials as photoconductors,[2] photoreceptors[3] and optical recording media.[4]

Compact laser beam printers (LBPs) equipped with GaAlAs laser diodes that emit radiation at wavelengths beyond 750 nm have been introduced. Although a number of inorganic photoconductors, including amorphous selenium, cadmium sulfide, and zinc oxide, have been used as photoconductors for electrophotography, these photoconductors all have photosensitivity principally in the visible region, so that they are useful in conventional copying machines. Photoreceptors with photoresponse in the near-IR region of 760–830 nm are, however, needed for LBP applications. For this reason, active research is under way on dual-layered photoreceptors using organic materials, such as phthalocyanines, for LBP applications.

A schematic of a multilayered photoreceptor, which is constructed with a thin charge generation layer (CGL) contiguous with a charge transport layer (CTL), is shown in Fig. 1. This structure is the principal type used in commercial organic photoreceptors so far. In general, they are prepared by dispersing photoconductive pigments in a solution with polymer binder and coating the dispersion onto a conductive substrate to form a CGL on a commercial base. Vacuum-deposited CGLs are also used for trivalent or tetravalent metal complexes with phthalocyanine.

Photosensitivity has been reported to depend on the specific crystal form of phthalocyanine used. We have investigated photosensitivity of the ϵ-form copper phthalocyanine (ϵ-CuPc)[5] and the τ-form metal-free phthalocyanine (τ-H_2Pc)[6] for charge generation materials of photoreceptors for LBPs. A photoreceptor incorporating dispersed ϵ-CuPc particles was found to exhibit near-IR photosensitivity of 32 ergs/cm^2 half-decay sensitivity ($E_{1/2}$) at 760 nm[5]; for one incorporating τ-H_2Pc, $E_{1/2}$ was 5 ergs/cm^2.[6]

Trivalent or tetravalent metal complexes with phthalocyanines have, moreover, been reported to be of promise for charge generation materials. Chloroaluminum phthalocyanine (AlPcCl),[7,8] chloroindium phthalocyanine (InPcCl),[9–11] oxovanadium phthalocyanine (VOPc),[12] and oxotitanium phthalocyanine (TiOPc)[13–16] have all been utilized in highly sensitive devices. For instance, the near-IR photosensitivity of a dual-layered photoreceptor with vacuum-deposited chloroaluminum chlorophthalocyanine (Cl_nAlPcCl) and pyrazoline for charge transport material was 4 ergs/cm^2 at 825 nm,[8] and that of a photoreceptor with InPcCl and a *N*,*N*′-diphenyl-*N*,*N*′-bis(3-methylphenyl)-[1,1′-biphenyl]-4,4′-diamine (TPD) for charge transport material was approximately 3 ergs/cm^2 in the 800–850 nm region.[11] A dual-layered photoreceptor using VOPc, with the CGL on top of the CTL, exhibited high photosensitivity in the near-IR region.[12]

IR-sensitive photoreceptors using TiOPc dispersed in a polymer have been actively investigated as CGLs. The crystal structure of TiOPc, which has α-(triclinic) and β-(monoclinic) forms, has been determined by Hiller et al.[13] Differen-

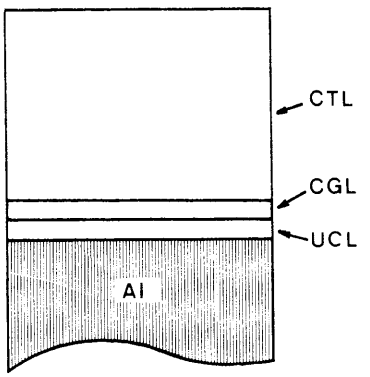

Figure 1. Cross-sectional view of a multilayered photoreceptor.

Received Apr. 27, 1990; revised Aug. 6, 1990.

Printed in U.S.A.

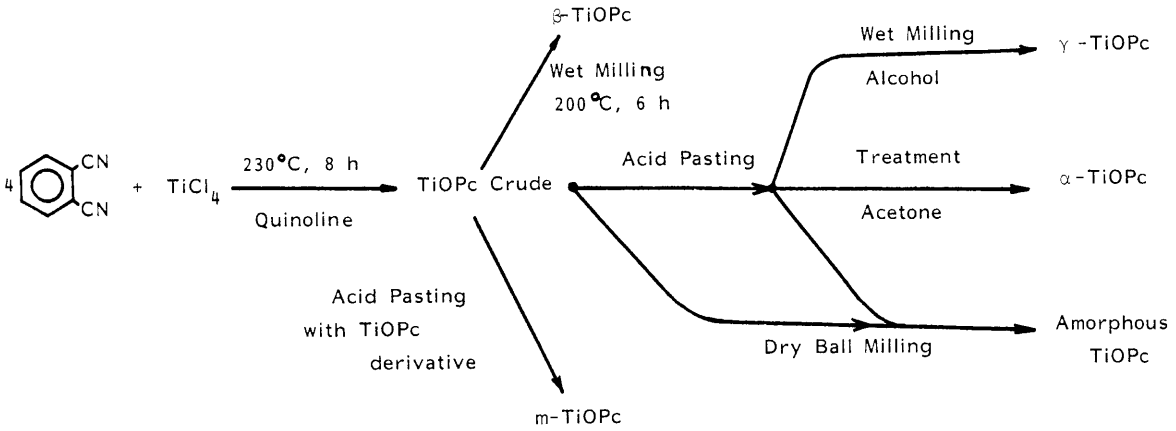

Scheme I. Processes for treatment of oxotitanium phthalocyanines.

tial scanning calorimetry (DSC) indicated the transformation from the α-form to the β-form at 230°C, with a change in enthalpy of −20 J/g.[14] A photoreceptor with α-TiOPc and a hydrazone derivative exhibited photosensitivity of 2.7 ergs/cm^2 at 830 nm,[15] and one of β-TiOPc and hydrazone showed approximately 4 ergs/cm^2.[16] Recently, m-TiOPc, which was distinguished from the α- and β-forms, has been developed for a photoreceptor device.[14] The photosensitivity of the m-form was 2.4–3.0 ergs/cm^2 in the 600–830 nm region.

In this paper, we describe the polymorphism of TiOPc. Five polymorphs, including amorphous- and γ-forms, are characterized by means of x-ray powder diffractometry, spectrophotometry and electron spin resonance (ESR) spectroscopy. Also, applications of the TiOPc polymorphs as charge generation materials in photoreceptors for printers are reported.

Experimental

Preparation of TiOPc. Crude TiOPc was synthesized by the reaction of phthalonitrile (25.6 g: 0.2 mol) and titanium tetrachloride (9.5 g: 0.05 mol) in 200 g of quinoline at 210°C for 8 hr. The resulting product was purified by washing in succession with hot quinoline at 130°C, 3% ammonium hydroxide, 3% hydrochloric acid, acetone and ethanol. Following the process for crystal transformation of TiOPc shown in Scheme I, β-TiOPc was prepared from crude TiOPc by wet milling in quinoline at 200°C for 6 hr.

m-TiOPc was produced as follows: Crude TiOPc and a TiOPc derivative were added to concentrated sulfuric acid, and that solution was poured into distilled water. In this experiment, the derivative used was octachloro-TiOPc. Conversion to the m-form was achieved by wet milling for 10 hr. α-TiOPc was prepared from crude TiOPc by acid-pasting and treatment with acetone. γ-TiOPc was prepared from acid-pasted TiOPc by wet milling in n-butyl alcohol. Amorphous TiOPc was prepared by dry milling acid-pasted TiOPc for a week. All polymorphs were assayed by x-ray powder diffraction. Further purification was performed by solvent-extraction methods. Other chemicals used were obtained from Toyo Ink Mfg. Co., Ltd., without further purification.

Analytical Measurements. Molecular weight of TiOPc crystals was measured by a Hitachi M-300-FD mass spectrometer. Average particle size of phthalocyanines was determined by a Shimadzu SA-CP3 centrifugal particle analyzer, which measured particles dispersed in THF. X-ray diffraction patterns of TiOPc were recorded on a Rigaku x-ray powder diffractometer RU-200, using CuKα monochromatic radiation. Absorption spectra were measured on a Shimadzu UV-365 spectrophotometer, using thin films of TiOPc dispersed in a polymer binder. IR spectra of pigments

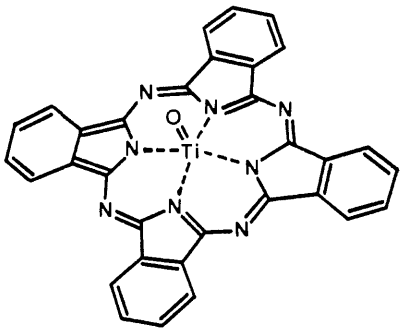

(a)

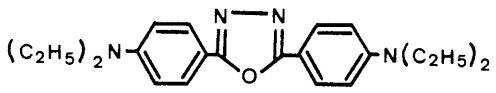

1) Oxadiazole

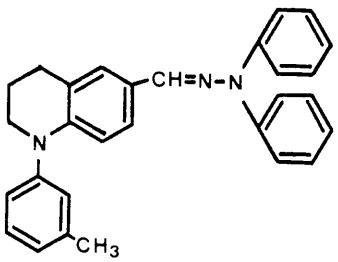

2) Hydrazone

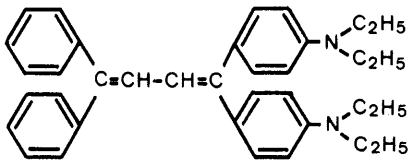

3) Butadiene

(b)

Figure 2. Structures of (*a*) charge generation materials and (*b*) charge transport materials.

dispersed in KBr pellets were measured on a JEOL Fourier Transform Infrared Spectrometer JIR-100 with a grating monochromator. Polystyrene and indene served as standards. ESR measurements of powder samples were performed at room temperature, using a JEOL JES-FE-1XG X-band Spectrometer with 100-kHz field modulation. Powder was sealed in a glass capillary tube and attached between the magnets. Ionization potentials (I_p) of powder samples were measured by a Riken-keiki AC-1 photoelectron emission spectrometer in air at room temperature. Hole drift mobilities of the charge transport materials were measured by the time-of-flight technique, using a Xe-flash pulse irradiated on a positively biased NESA glass under 10^{-3} torr at 5 $\times$ 10^5 V/cm.

Electrophotographic Measurements. Materials used for the CGL and the CTL are shown in Fig. 2. The charge generation materials are the five forms of TiOPc, and the charge transport materials are 2,5-bis(*p*-diethylaminophenyl)oxadiazole ("oxadiazole"), 1-(3-methylphenyl)-1,2,3,4-tetrahydroquinoline-6-carboxyaldehyde-1′,1′-diphenylhydrazone ("hydrazone"), and 1,1-bis(*p*-diethylaminophenyl)-4,4-diphenyl-1,3-butadiene ("butadiene"), respectively.

Electrophotographic measurements are obtained for photoreceptor devices on substrate. The substrate is a 100-μm aluminum plate coated with a 0.7 μm polyamide resin undercoat layer (UCL). Each CGL consists of 50 wt % TiOPc dispersed in poly(vinylbutyral) resin, with thickness 0.10 μm. The CTL was composed of 50 wt % charge transport material prepared by dissolving in bisphenol-A polycarbonate and methylene dichloride and coating onto the CGL at thickness of 20 μm.

The electrophotographic measurements were made by a Kawaguchi Electric EPA-8100 Electrophotographic paper analyzer, using a halogen-lamp light source. The wavelength was selected by a monochromator or by interference filters. Photoinduced discharge curves were measured in terms of surface potential versus time. The measurements were run so that there was a charge, a 2-sec dark decay period, and a 3-sec white-light exposure period. V_0 is the initial dark potential before white light irradiation, DD is the average potential of dark decay for 2 sec, $E_{1/2}$ and $E_{1/5}$ are the exposure for surface potential to a half-decay and one-fifth decay exposure, respectively, and V_{r3} is the residual potential at 3 sec after exposure. The values of V_0 were adjusted to 600 $\pm$ 10 (−V) by control of the applied corona charge.

The spectral sensitivity was determined by the half-decay of the surface potential at −800 V due to 20 ergs/cm^2 exposure from 450 to 850 nm. Curves of surface potential versus exposure were obtained by a computer-controlled electrophotographic cycling system, using a corotron wire for charging. The surface potential was measured by an electrostatic voltmeter (362A: Trek Corp.) at various exposures. Initial voltage was determined at −800 V. White light was passed through an interference filter and a colored band pass filter, in order to obtain 790-nm light.

Results and Discussion

FD mass spectrometry showed a single peak corresponding to M^+ (*m/z* of 576) assigned to TiOPc. We concluded, therefore, that the crystals of these TiOPcs did not contain any other derivatives. Median diameter and specific surface area of TiOPcs are shown in Table I, together with corresponding data for other well-known phthalocyanines used for charge generation materials. The four crystalline polymorphs of TiOPc and the X-H_2Pc have almost the same particle size, 0.08 $\pm$ 0.01 μm, compared with 0.13 μm for ϵ-CuPc and 0.21 μm for τ-H_2Pc. Amorphous TiOPc was appreciably smaller than the crystalline polymorphs of TiOPc. These results suggest the feasibility of CGL formation with well-aligned particles and also imply a decrease in the space charge at the interface between CGL and CTL.

TABLE I. Average Particle Size and Specific Surface Area of Phthalocyanines[a]

Phthalocyanine	Median diameter, μm	Specific surface area, m^2/g
Amorphous TiOPc	0.05	117
α-TiOPc	0.08	57
β-TiOPc	0.09	61
γ-TiOPc	0.07	71
m-TiOPc	0.09	67
X-H_2Pc	0.07	78
τ-H_2Pc	0.21	23
ϵ-CuPc	0.13	35

[a] These values were measured by the centrifugal particle analyzer. The particles were dispersed in THF.

Polymorphism of TiOPc

X-ray Powder Diffraction. The x-ray powder diffraction patterns indicate, within limits, what lattice defects or crystal transformations are formed, which depends upon the conditions in the manufacture of the TiOPc crystals. The x-ray powder diffraction data of the five polymorphs of TiOPc are shown in Fig. 3 and Table II. Positions and intensities of the diffraction lines are identified for the five polymorphs. Although the crystal orientations for the amorphous, γ- and *m*-forms have not yet been determined, the structures of the α- and β-forms have been analyzed by a four-circle diffractometer.

Based on the x-ray powder diffraction, the orientations of the (010) face in the α-form and the (001) face in the β-form are very high compared with the other faces. In the DSC analysis the α-form shows an exothermic peak at 230°C, attributed to crystal transformation from the α-form to the β-form.[14] This means that the β-form is thermodynamically stable.

Although the crystal structures of the γ- and *m*-forms are not known, their x-ray diffraction patterns have strong lines. The γ-form shows intense peaks at 2θ = 7.3, 17.7, 24.0, 27.2, and 28.6°, corresponding to interplanar distances of 12.1, 5.0, 3.71, 3.28, and 3.12 Å, respectively. The characteristic peak at 27.2° (3.28 Å) was the strongest of all, suggesting a state of stacked TiOPc molecules that depends on the crystal conversion by wet milling in a polar solvent (*n*-butylalcohol). Furthermore, the γ-form does not have any well-defined peaks in the range of 8–17°. On the other hand, the *m*-form has three intense peaks, at 2θ = 6.9, 15.5, and 23.4°, respectively, corresponding to interplanar distances of 12.8, 5.7, and 3.80 Å. The characteristic interplanar distance of 3.80 Å for the *m*-form distinguishes it from the other polymorphs, and this rather long distance should be attributed to the use of the substituted TiOPc derivative in the acid pasting process. The amorphous TiOPc has no definite peaks, indicating that it is not stacked regularly.

Absorption Spectra. Absorption spectra of TiOPc particles dispersed in films and of TiOPc dissolved in 1-chloronaphthalene are shown in Fig. 4. The absorption spectrum of the solution of TiOPc shows a narrow absorption peak, with molecular extinction coefficient $\epsilon = 4.42 \times 10^5$ L/mol · cm, at 700 nm. This result indicates that TiOPc is present as isolated molecules in 1-chloronaphthalene. The absorption spectrum of CuPc in 1-chloronaphthalene also showed a narrow peak, with $\epsilon = 7.31 \times 10^4$ L/mol · cm, at 676 nm. These results can be explained by Davydov's theory of molecular extinction, and the magnitudes of the allowed transition splitting are confirmed from measurements of the intermolecular forces—that is, the exciton splitting for Ti=O in TiOPc is larger than that of Cu in CuPc.

Solid-state absorption peak data of the TiOPc polymorphs are listed in Table III. As shown in Fig. 4, the absorption peaks for the amorphous, α-, β-, and *m*-forms are broad-

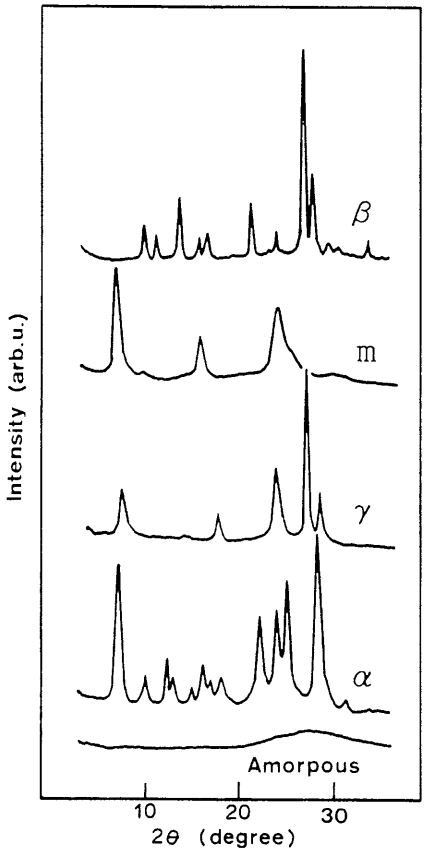

Figure 3. X-ray powder diffraction patterns of oxotitanium phthalocyanines.

TABLE II. X-Ray Powder Diffraction Angles and Peak Intensities for Oxotitanium Phthalocyanines

(*a*) α- and β-TiOPc

α-TiOPc				β-TiOPc			
2θ (°)	d(Å)	(hkl)	I/I_0	2θ (°)	d(Å)	(hkl)	I/I_0
7.6	11.6	(010)	86	9.4	9.4	(011)	24
10.3	8.6	(001)	23	10.6	8.3	(11$\bar{1}$)	19
12.7	7.0	(101)	34	13.3	6.7	(10$\bar{2}$)	37
13.3	6.7	(011)	23	15.2	5.8	(210)	18
16.3	5.4	(111)	30	15.7	5.6	(12$\bar{1}$)	15
18.4	4.8	(20$\bar{1}$)	24	16.2	5.5	(102)	19
22.7	3.92	(012)	57	21.0	4.2	(013)	36
24.3	3.66	(21$\bar{2}$)	63	23.5	3.80	(113)	18
25.5	3.50	($\bar{2}$02)	79	26.5	3.35	(001)	100
28.8	3.11	($\bar{2}$12)	100	27.4	3.25	(014)	47
				28.5	3.14	(33$\bar{1}$)	11

(*b*) γ- and *m*-TiOPc

γ-TiOPc			*m*-TiOPc		
2θ (°)	d(Å)	I/I_0	2θ (°)	d(Å)	I/I_0
7.3	12.1	36	6.9	12.8	100
17.7	5.0	25	15.5	5.7	47
24.0	3.71	46	23.4	3.80	70
27.2	3.28	100			
28.6	3.12	36			

ened and split into two bands. The band splittings of the amorphous, α-, β-, and *m*-forms are 3303, 3528, 2903, and 2237–4081 cm^{-1}, respectively. These splittings can be explained by the formation of dimers of phthalocyanine molecules and indicate strong intermolecular interaction between them. Similar phenomena indicate that *X*- and τ-form H_2Pc form dimeric structures or associate into

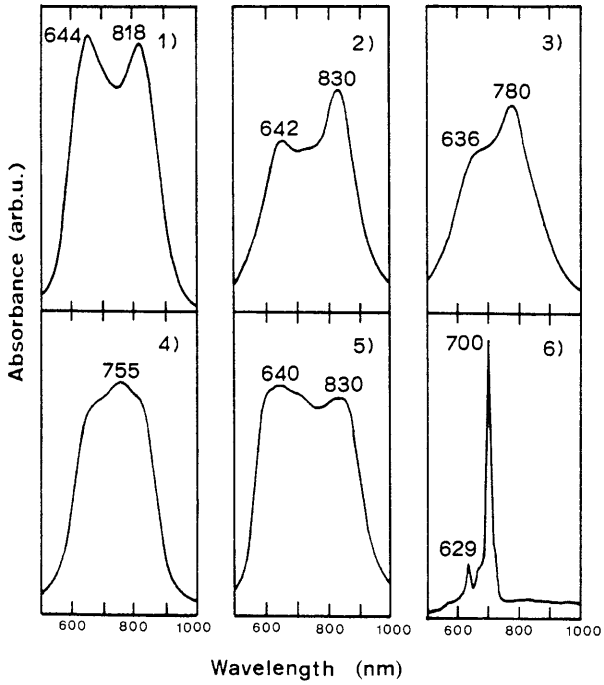

Figure 4. Absorption spectra of oxotitanium phthalocyanines coated on glass with a binding polymer and in solution in 1-chloronaphthalene. The films are 0.2 μm thick. The films are (1) amorphous, (2) α-form, (3) β-form, (4) γ-form, (5) *m*-form; (6) is a solution spectrum of TiOPc in 1-chloronaphthalene.

TABLE III. The Wavelengths (nm) of Absorption Peaks of Oxotitanium Phthalocyanines

Amorphous	α	β	γ	*m*	Dissolved TiOPc[a]
644	642	636	660	620–700	629, 666
			755		700
818	830	780	815	830	

[a] In 1-chloronaphthalene.

molecular aggregates.[3,6] The γ-form of TiOPc, however, has a maximum peak at 755 nm, which does not indicate a large splitting into two bands. This peak at 755 nm is a characteristic not shared with the other polymorph spectra, and it suggests the formation of an aggregate.

IR Spectra. Several IR spectroscopic investigations of metallophthalocyanines have been carried out to study the crystal forms.[17] The different crystal forms of TiOPc are characterized by somewhat different IR spectra. IR absorption spectral data of the five TiOPc polymorphs are shown in Fig. 5 and Table IV. Let us try to give an interpretation to the individual absorption lines in the spectra, based on the comparison of their vibrational frequencies. Slight differences are apparent in the regions of 700–800 and 1600–2000 cm^{-1}. In the region 700–780 cm^{-1}, the frequencies are assigned to (1) γ-C–H (719–732 cm^{-1}), (2) δ-C_6H_6 (~750 cm^{-1}), (3) ν-C–N (770–780 cm^{-1}); therefore, we can recognize the polymorphism in comparing the five crystals.

In particular, the two frequencies of (3) are unique for each polymorph; that is, these frequencies depend on the orientation of the planar phthalocyanine molecules, and the bands of longer wavenumber of thermodynamically stable polymorphs appear more intense than those of unstable polymorphs. We can confirm that the β-form is the most stable polymorph, and the bands are sharp due to well-stacked molecular interactions. On the contrary, the bands of the amorphous form are very broad, due to its irregular crystal orientation. Differences in the polymorphs in the

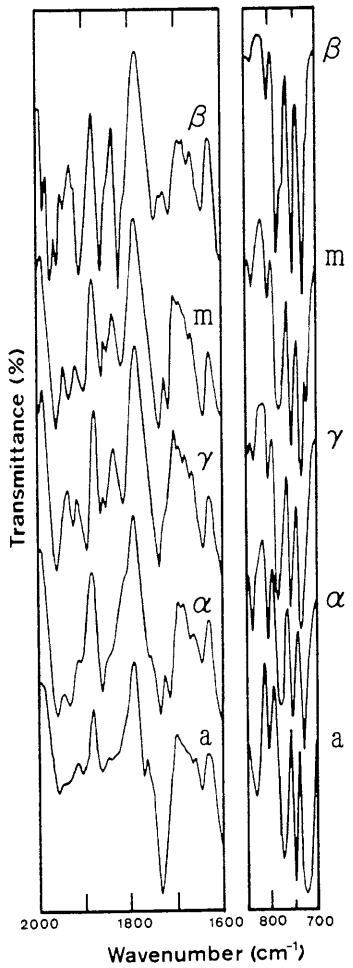

Figure 5. IR absorption spectra (cm^{-1}) of oxotitanium phthalocyanines.

TABLE IV. IR Absorption Spectra (cm^{-1}) of Oxotitanium Phthalocyanines

Amorphous	α	β	γ	m
				719
728	728	732	728	729
752	752	752	752	751
780	780	776	779	777
	783	784		
1609	1609	1609	1609	1609
1646	1646	1644	1645	1645
1670	1668	1671	1670	1672
	1715	1712	1718	1710
1735	1734	1743	1739	1735
1773	1762		1814	1815
1830		1822	1849	1822
1864	1864	1861	1864	1870
		1896	1894	1897
1908	1911			
1934	1942	1940	1925	1938
1957	1958	1956	1960	1962
		1968		
		1985		

wavelength range 1600–2000 cm^{-1} are also found. Here the well-stacked polymorphs have well-split intense bands between 1800 and 2000 cm^{-1}, and the intensities of the bands in the 1700–1750 cm^{-1} range become weak. As a result of these measurements, the order of the well-packed polymorphs can be compared from the top to the bottom in this figure; the decrease occurs in that order. The absorption line at 1609 cm^{-1} probably corresponds to the valence vibration of the C–C conjugated bonds of the benzene rings.

ESR Spectra. ESR spectroscopy has been applied to characterization of the polymorphs of H_2Pc by Harbour et al.[18] There are many strains and defects in the phthalocyanine particles, where either electrons or holes may accumulate. The ESR spectra relate to the bonding of the central Ti=O with the surrounding four isoindole nitrogen atoms, without additional information from the rest of the molecule. The molecular centers in the solid are located at the lattice point, so that the molecules cannot rotate in the particle; that is, the g-factors and hyperfine coupling constants reflect the magnitude of anisotropy in the crystal structure.

ESR spectra and the parameters of powder TiOPc are shown in Fig. 6 and Table V, respectively. Differential signals due to the conduction band electrons for TiOPc are intense and narrow, and the Lorentzian curves appear at approximately 2.0014 (g-factor) with 3.8–5.0 G (ΔH_{pp}), in which the characteristic hyperfine structure resulting from the signals of ^{47}Ti can be seen in their splitting. The g-factors of the α-, γ-, and m-forms have the same values (2.0014), that of the β-form is smaller (2.0012), and that of the amorphous is larger (2.0015). Because the g-factor represents the degree of disorder, these results suggest a structure having greater disorder for the amorphous TiOPc and a well-ordered structure for the β-form. The ΔH_{pp} values depend on $n^{-1/2}$, where n is equal to the number of molecules over which the unpaired electron is delocalized.[17] The ΔH_{pp} of the m-form is larger than those of the other polymorphs, and this difference may be the result of localization of the orientation of the m-TiOPc molecules and the use of the TiOPc derivative in the process of manufacture. On the contrary, the ΔH_{pp} values of the other four polymorphs are almost equal; therefore, the extent of localization won't be very different.

ESR line shape also reflects the environment and nature of the TiOPc polymorphs (Fig. 6). In the case of amorphous TiOPc, the spectrum consists of an isotropic line. This result can be explained by the delocalization of electrons/holes in TiOPc molecules for the amorphous state in a particle. Furthermore, the ESR spectrum of the α-form shows the characteristic eight hyperfine splittings due to the spin of $I = 7/2$ of ^{47}Ti. Many sharp lines can also be seen superimposed on some of the eight resonance lines, especially on either side of the large line for the conduction band. These sharp lines reflect the interaction of ^{14}N and ^{47}Ti in the phthalocyanine molecules. Because the α-form has a triclinic structure and the Ti=O in the molecules is arranged in the same direction along the axis, the hyperfine structure due to the central Ti=O can be measured more easily than the other structures. As a result, the magnitude of the resonance lines decreases for the α-, γ-, and m-forms in this order. It is, therefore, presumed that the order of the Ti=O arrangement becomes weaker than that of the α-form. On the contrary, the ESR line of the β-form is quite different from that of the other polymorphs; that is, no hyperfine resonance line due to ^{47}Ti is found in the spectrum. Instead of those lines, the β-TiOPc has complicating lines like H_2Pc without the hyperfine structure resulting from the metal. Molecules of the β-form have an alternate up-and-down arrangement influenced by the spin of ^{47}Ti, and only the essential spins of the phthalocyanine molecules can be detected.

Electrophotographic Measurements

Discharge Measurement. Photoinduced discharge curves (PIDCs) of multilayered photoreceptors using the five polymorphs of TiOPc as charge generation materials (CGM) and (1) oxadiazole, (2) hydrazone, and (3) butadiene derivatives as charge transport materials (CTM) are summarized in Table VI. The values of ionization potential (I_p)

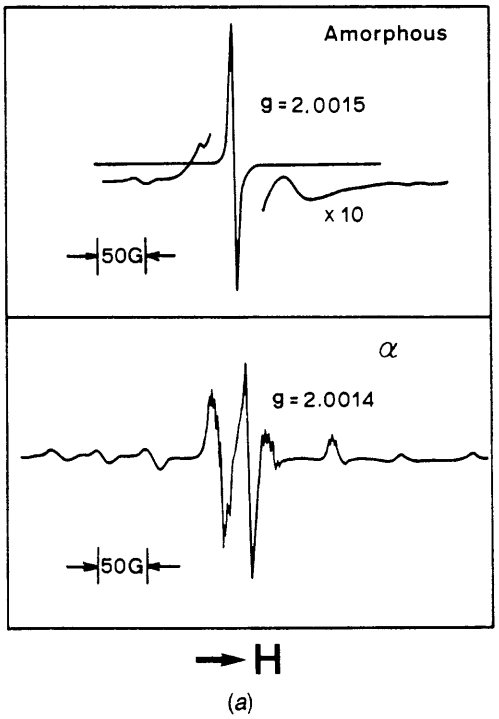

(a)

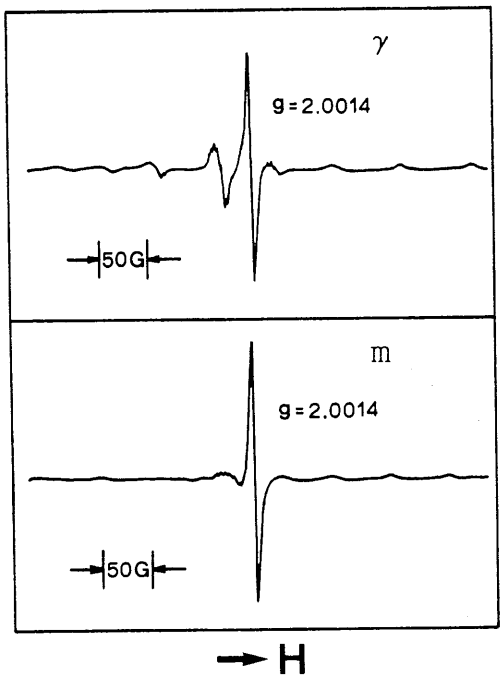

(b)

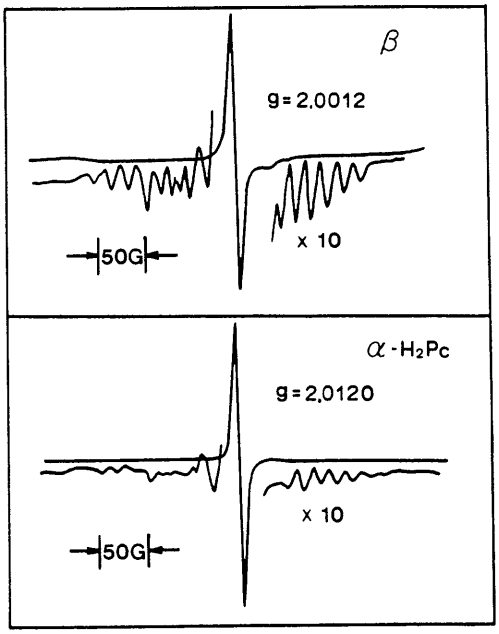

(c)

Figure 6. ESR spectra of powder samples of phthalocyanines.

TABLE V. ESR Parameters for Oxotitanium Phthalocyanines

Polymorph	*g*-factor	ΔH_{pp}, G
Amorphous	2.0015	4.0
α	2.0014	3.8
β	2.0012	4.0
γ	2.0014	4.1
m	2.0014	5.0
α-H_2Pc	2.0120	5.8

TABLE VI. Electrophotographic Values of Discharge Measurement

White light (400–700 nm)[a]			Light intensity: 5 lux		
TiOPc	V_0, −V	*DD*, V/sec	$E_{1/2}$, lux · sec	$E_{1/5}$, lux · sec	V_{r3}, −V
Amorphous	599	28	0.6	0.9	0
α	600	48	0.7	1.4	12
β	607	28	1.1	2.3	3
γ	607	30	0.5	0.8	1
m	603	42	0.6	1.0	3

[a] V_0 is the initial dark potential before white light irradiation, *DD* is the average potentials of dark decay, for 2 sec, $E_{1/2}$ and $E_{1/5}$ are the exposures for surface potential to a half and one-fifth, respectively, V_{r3} is the residual potential at 3 sec after exposure. The values of V_0 are adjusted to 600 ± 10 (−V) with the control of applied corona charge.

TABLE VII. The Ionization Potentials (I_p) and Mobility (μ)

Material	I_p, eV	μ, cm²/V · sec[a]
TiOPc		
amorphous	5.39	—
α	5.34	—
β	5.27	—
γ	5.38	—
m	5.35	—
CTM		
(1) oxadiazole	5.74	5.7×10^{-8}
(2) hydrazone	5.17	1.2×10^{-6}
(3) butadiene	5.11	8.7×10^{-6}

[a] The mobility is measured by time-of-flight technique with Xe flash at 5×10^5 (V/cm).

and mobility (μ) are shown in Table VII. The photoreceptors exhibit low dark decay, good white-light sensitivity, and low residual potential. Because the three derivatives used for CTM have different mobilities, the sensitivity results appear in the order 3 > 2 > 1. The ability of charge transport in CTL and the facility of charge injection from CGL to CTL are predictable from the values of I_p for CTM. Furthermore, the photoreceptors using amorphous TiOPc or γ-TiOPc exhibit slightly better sensitivities. The order of sensitivity will be as follows: γ ≧ amorphous > *m* > α > β. This result is also approximately dependent on the order of the I_p values for CGM.

Although the photoreceptor using the oxadiazole derivative for CTM exhibits lower sensitivity and higher residual

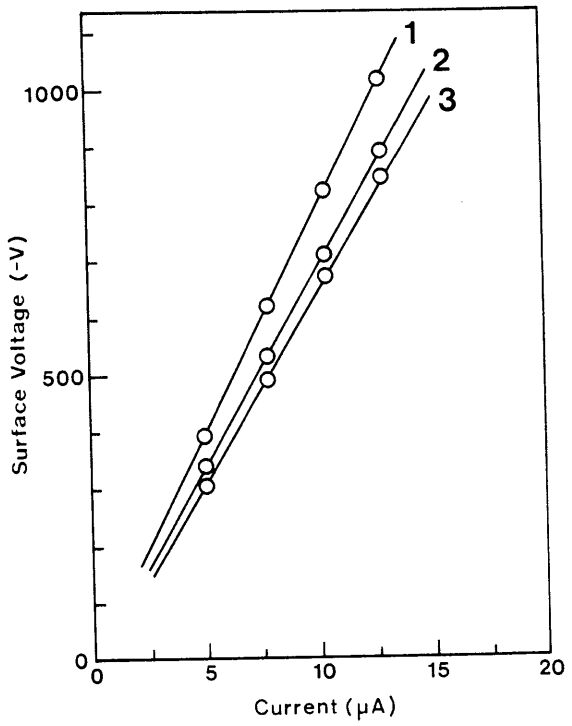

Figure 7. Surface potentials of amorphous-TiOPc photoreceptors versus applied current.

potential, higher surface potential and lower dark decay are also observed at the same time. These tendencies are due to the lower mobility of the oxadiazole derivative. Furthermore, the existence of many traps result from the structural reason would consider.

Surface potentials of amorphous-TiOPc photoreceptors using the three kinds of CTM are shown in Fig. 7. The potentials yield straight lines with applied current, and the potentials decrease in the order oxadiazole, hydrazone, butadiene. This result may also indicate that the holes separated from electrons in the CGL are injected most rapidly into the CTL with the CTM using the butadiene derivative, which has a large resonance overlap for high mobility and good injection efficiency. The residual electrons in the CGL, which move into the aluminum substrate through the UCL, are neutralized by the positive charge of the substrate. This phenomenon gives rise to the lowering of the surface potential of the photoreceptor.

Spectral Sensitivity Measurement. Spectral sensitivities of the photoreceptors from 450 to 850 nm, using the five polymorphs of TiOPc as charge generation materials and the three derivatives for charge transport materials, are shown in Fig. 8. The photoreceptors exhibit good sensitivity in the 600–800-nm region. The spectral responses are dependent on the absorption spectra of the CGL films, and the sensitivities are affected by the mobility of the CTM. The spectral sensitivity of photoreceptors using the butadiene derivative for the CTM decreases rapidly below 500 nm because the incident light is absorbed in the CTL, the absorption maximum of the butadiene derivative being at 400 nm. The amorphous and *m*-form TiOPc each show two absorption maxima at 830 and 600 nm. The α- and β-forms show single absorption peaks at 830 and 780 nm, respectively. The photoreceptors incorporating the γ-form are panchromatic from 600 to 800 nm, with good spectral sensitivity throughout this range.

Surface Potential versus Exposure. Figure 9 and Table VIII show photosensitivity plots and a summary of electrophotographic electrical values of multilayered photoreceptors, again using the five forms of TiOPc for CGM and the three derivatives for CTM, for 790-nm light exposure. Al-

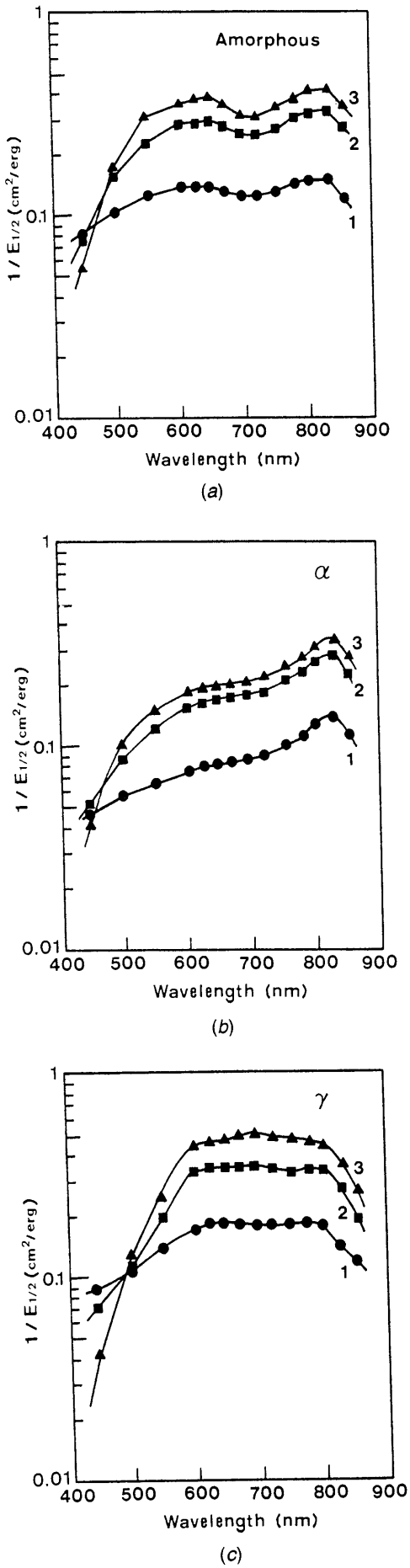

Figure 8. (*Continued on next page with caption*).

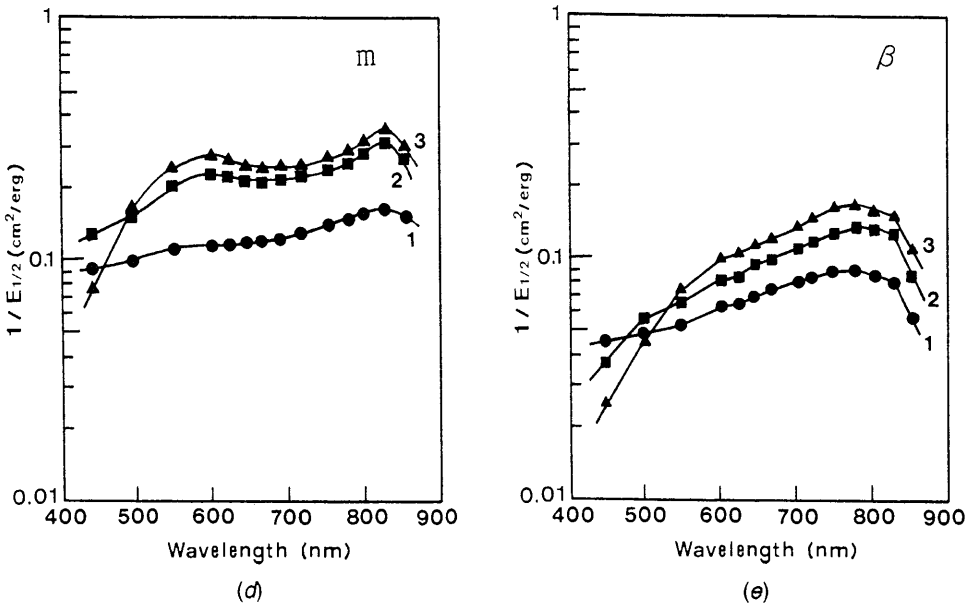

Figure 8. Spectral sensitivities of oxotitanium phthalocyanines.

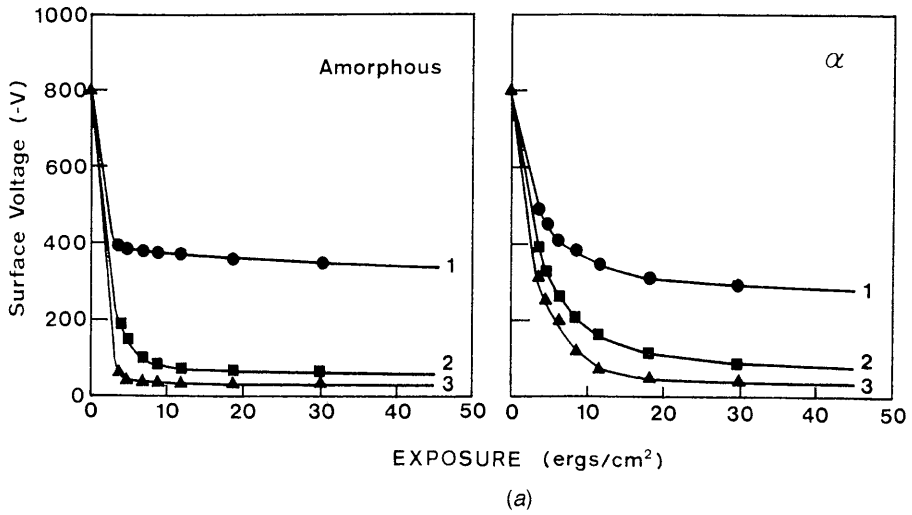

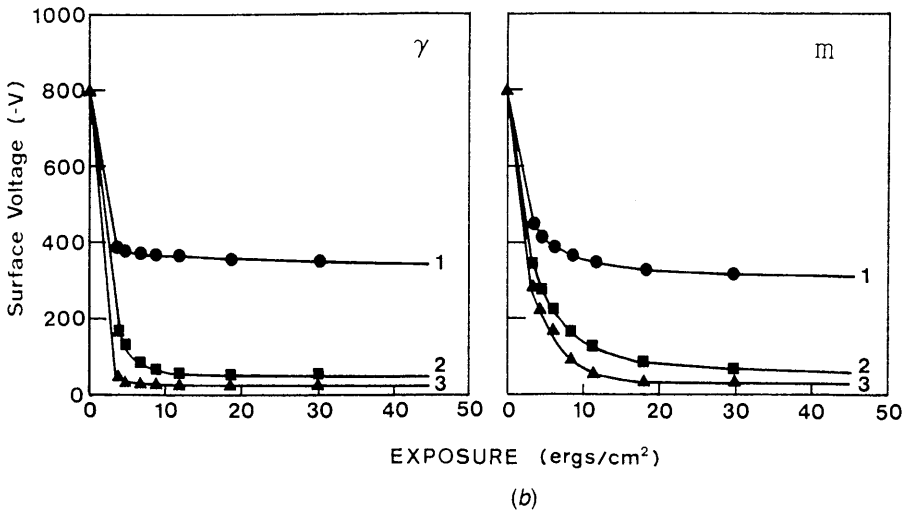

Figure 9. (*Continued on next page with caption*).

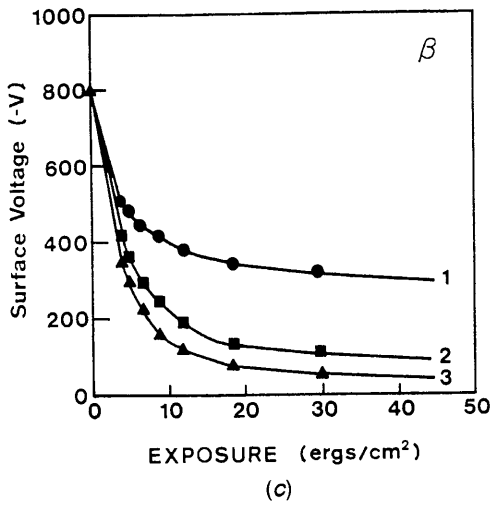

Figure 9. Surface potential versus exposure curve for oxotitanium phthalocyanine and charge transport material multilayered photoreceptors. CTM: (1) oxadiazole, (2) hydrazone, and (3) butadiene.

TABLE VIII. Electrophotographic Characteristics of Multilayered Photoreceptors at 790 nm

TiOPc polymorph	Amorphous	α	β	γ	m
	(1) Oxadiazole derivative				
Dark decay, V/sec	28	38	17	26	33
$E_{1/2}$, erg/cm^2	3.5	7.2	10.3	3.7	5.8
Surface voltage at 5 erg/cm^2, −V	380	455	475	375	405
Surface voltage at 10 erg/cm^2, −V	370	365	400	360	360
Surface voltage at 30 erg/cm^2, −V	345	300	325	350	320
	(2) Hydrazone derivative				
Dark decay, V/sec	45	55	35	44	50
$E_{1/2}$, erg/cm^2	2.3	3.7	4.3	2.7	3.0
Surface voltage at 5 erg/cm^2, −V	140	315	370	120	265
Surface voltage at 10 erg/cm^2, −V	80	165	225	60	135
Surface voltage at 30 erg/cm^2, −V	65	90	115	50	70
	(3) Butadiene derivative				
Dark decay, V/sec	58	65	45	54	60
$E_{1/2}$, erg/cm^2	1.9	2.6	3.6	1.8	2.4
Surface voltage at 5 erg/cm^2, −V	40	230	290	35	195
Surface voltage at 10 erg/cm^2, −V	35	100	140	30	75
Surface voltage at 30 erg/cm^2, −V	30	40	55	25	30

though the residual voltages of the photoreceptors using the oxadiazole derivative exhibit large values, the photoreceptors using the other two derivatives exhibit good sensitivity at 790 nm. The dark decay, the energy required to produce 50% discharge from the initial potential before light irradiation ($E_{1/2}$) and the surface voltage on exposure of 5, 10, and 30 ergs/cm^2 are shown in Table VIII. When a given TiOPc is used for CGM, the photosensitivity decreases in the order (3) butadiene, (2) hydrazone, and (1) oxadiazole. Dark decay also decreases in this order. The order of sensitivity of the CGMs is $\gamma \geqq$ amorphous $> m > \alpha > \beta$, corresponding to the order of the PID curves.

In particular, the γ-TiOPc/butadiene photoreceptor exhibits a dark decay = 54 V/sec, $E_{1/2}$ = 1.8 ergs/cm^2, and surface voltage at 5 ergs/cm^2 = −35 V, at 10 ergs/cm^2 = −30 V, and at 30 ergs/cm^2 = −25 V for exposure at 790 nm. Furthermore, the amorphous TiOPc/butadiene photoreceptor exhibits almost the same electrical values. These data indicate that the high charge carrier generation efficiency of TiOPc, especially with the γ-form and the amorphous particles dispersed in polymer binder, and the high charge transport ability result from the high hole-drift-mobility of 1,1-bis(*p*-diethylaminophenyl)-4,4-diphenyl-1,3-butadiene. In the case of amorphous TiOPc, recrystallization may occur on the surface of the CGL film wet by methylene dichloride when the CTL is coated onto the CGL. We presume that recrystallization of TiOPc particles facilitates efficient injection of carriers from CGL to CTL. The γ-form has a structure for excellent injection of the carrier; the structure forms in the process of γ-form crystal preparation. On the contrary, the β-form, in which there is alternate arrangement of the direction of the Ti:O bonds, will inhibit carrier generation and transport in the CGL. In spite of the different crystal forms of TiOPc, all photoreceptors incorporating TiOPc for CGM exhibit high sensitivity in the 600–800-nm region because of the extended vacant *d*-orbitals perpendicular to the phthalocyanine molecule.

Conclusions

We have investigated five polymorphs of TiOPc from the viewpoint of structural, spectroscopic and magnetic properties, and studied their application as the CGM of photoreceptors for laser beam printers. As a result of the experiments, the differences in the polymorphs were clarified. Furthermore, the multilayered photoreceptors exhibited high sensitivity in the IR wavelength region, low dark decay and low residual potentials.

Acknowledgment. The authors would like to acknowledge the support of Toyo Ink Mg. Co., Ltd.

References

1. F. H. Moser and A. L. Thomas, *Phthalocyanine Compounds*, Reinhold Publishing Corp., New York, 1963; F. H. Moser and A. L. Thomas, *The Phthalocyanines*, CRC Press, Florida, 1983.
2. F. Gutmann and L. E. Lyons, *Organic Semiconductors*, J. Wiley & Sons, New York, 1967; H. Meier, *Organic Semiconductors*, Verlag Chemie, Berlin, 1974; J. Simon and J. J. Andre, *Molecular Semiconductors*, Eds. C. W. Rees and J. M. Lehn, Springer, Berlin, 1985.
3. J. Wiegl, J. Mammino, G. L. Whittaker, R. W. Radler, and J. F. Byrne, *Current Problems in Electrophotography*, W. F. Berg and K. Hauffe, Eds., Walter de Gruyter, Berlin, 1972, p. 287; M. Smith, R. Radler, and C. Hackett, UK Pat. 1,337,228(1973); P. J. Regensberger, UK Pat. 1,337,227(1973).
4. L. Alexandru, M. A. Hooper, R. O. Loutfy, J. H. Sharp, P. S. Vincett, G. E. Johnson, and K. Y. Law, *Mater. Microlithogr.* **22:** 435(1984).
5. M. Takada and M. Sawada, *Japan Koho* 1662(1977); T. Yagishita, K. Ikegami, T. Narusawa, and H. Okuyama, *IEEE Trans. Indust. Appl.* **1A-20:** 1642(1984).
6. S. Takano, T. Enokida, A. Kakuta, and Y. Mori, *Chem. Lett.* **1984:** 2037; A. Kakuta, Y. Mori, S. Takano, M. Sawada, and I. Shibuya, *J. Imaging Technol.* **11:** 7(1985); T. Enokida and S. Ehashi, *Chem. Lett.* **1988:** 179.
7. K. Arishima, H. Hiratsuka, A. Tate, and T. Okada, *Appl. Phys. Lett.* **40(3):** 279(1982).
8. S. Nogami, Y. Mori, and T. Iwabuchi, US Pat. 4,732,832(1988).
9. K. Kato, Y. Nishioka, K. Kaifu, K. Kawamura, and S. Ohno, *Appl. Phys. Lett.* **46:** 196(1984); US Pat. 4,426,434(1984).
10. P. M. Borsenberger, M. T. Regan, and C. F. Groner, US Pat. 4,471,039(1984).
11. R. O. Loutfy, C. K. Hsiao, A. M. Hor, and G. DiPaola-Baranyi, *J. Imaging Sci.* **29:** 148(1985); R. O. Loutfy, A. M. Hor, and A. Rucklidge, *J. Imaging Sci.* **31:** 31(1987).
12. S. Grammatica and J. Mort, *J. Appl. Phys.* **85:** 445(1981).
13. W. Hiller, J. Strahle, W. Kobel, and M. Hannack, *Z. Kristallogr.* **159:** 173(1982).
14. T. Enokida, R. Kurata, T. Seta, and H. Katsura, *Electrophotography* **27:** 533(1988).
15. K. Ohaku, H. Nakano, and M. Aizawa, US Pat. 4,728,592(1988).
16. T. Suzuki, T. Murayama, H. Ono, S. Otsuka, and M. Nozomi, US Pat. 4,664,997(1987).
17. A. A. Ebert and H. B. Gottlieb, *J. Am. Chem. Soc.* **74:** 2806(1952); D. N. Kendell, *Analyt. Chem.* **25:** 382(1953); A. N. Sidorov and I. P. Kotlyar, *Opt. Spectrosc.* **11:** 92(1961); B. I. Knudsen, *Acta Chem. Scand.* **206:** 1344(1966); T. Kobayashi, F. Kurokawa, N. Uyeda, and E. Suito, *Spectrochim. Acta* **26A:** 1305(1970).
18. J. H. Harbour and R. O. Loutfy, *J. Phys. Chem. Solids* **43:** 513(1982); J. R. Harbour and M. J. Walzak, *Langmuir* **2:** 788(1988).
19. R. L. Sasseville, J. B. Bolton, and R. O. Loutfy, *J. Phys. Chem.* **87:** 862(1983); R. L. Sasseville, A. R. McIntosh, J. R. Bolton, and R. O. Loutfy, *J. Phys. Chem.* **88:** 3139(1984).